Indonesian Journal of Electrical Engineering and Computer Science
Vol. 27, No. 2, August 2022, pp. 876~884
ISSN: 2502-4752, DOI: 10.11591/ijeecs.v27.i2.pp876-884

A novel singular value decomposition-based ultra wide band time-of-arrival estimation for multiple targets

Ibrahim Yassine Nouali[1], Zohra Slimane[2], Abdelhafid Abdelmalek[1]
[1]STIC Laboratory, Departement of Telecommunications, Faculty of Technology, Tlemcen University, Chetouane, Algeria
[2]STIC Laboratory, Department of Electrical Engineering, Belhadj Bouchaib University, Ain Temouchent, Algeria

Article Info

Article history:

Received Sep 20, 2021
Revised Jun 3, 2022
Accepted Jun 17, 2022

Keywords:

Multiple targets
Ranging
Singular value decomposition
Time-of-arrival
Ultra wide band

ABSTRACT

It is widely admitted that the estimation of ultra wide band (UWB) time-of-arrival (TOA) for multiple targets in indoor multipath channels is a very challenging task. The existing algorithms deal with a limited number of targets and require a complex exchange of several messages. In this paper, a novel TOA estimation algorithm for multiple targets is developed. The proposed algorithm estimates the first path (FP) TOA of a number of targets without exchanging messages or using collision avoidance techniques. As a first step, the singular value decomposition (SVD) is employed to extract the first path (FP) of each target and then a matched filter, followed by an iterative threshold crossing algorithm, is used to determine the number of targets and the corresponding FP TOAs. The simulation results with four targets, using the CM1 IEEE 802.15.4a channel model, showed that the proposed novel algorithm can effectively detect the FP of each target and estimate its corresponding TOA.

Corresponding Author:

Ibrahim Yassine Nouali
STIC Laboratory, Departement of Telecommunications, Faculty of Technology, Tlemcen University
Chetouane, Algeria
Email: ibrahimyassine.nouali@univ-tlemcen.dz

1. INTRODUCTION

Accurate information about indoor positioning is highly required for many applications such as navigation, surveillance, medical services, military applications and rescue operations. Many technologies, such as ultrasonic, infrared (IR), ultra wide band (UWB), Zigbee and wireless fidelity (Wi-Fi), have been developed and used for indoor positioning, depending on the application requirements in terms of accuracy and range [1]–[6]. Among all these technologies, UWB turned out to be the most promising because its large bandwidth allows for higher positioning accuracy, greater multipath resolution, better penetration capability and lower energy consumption [7]–[9].

In indoor range-based positioning systems a network of anchor nodes, with known coordinates (at least four anchors in three-dimensional localization), are deployed over an area that includes one or more targets. The target or the anchor nodes (in two-way ranging) emit a signal called ranging signal. This ranging signal involves various parameters, such as the time-of-arrival (TOA), strength, received signal strength (RSS), angle-of-arrival (AOA), which can be extracted and used to estimate the distance between the target and the anchor nodes [10]. In addition, the target position may be calculated by a simple application of geometric and trigonometric techniques. Owing to the large bandwidth of UWB signals, time-based parameters, such as the TOA, can be viewed as best suited for UWB-based indoor positioning since they can take full advantage of UWB characteristics [11].

The UWB TOA-based ranging method relies strongly on the detection of the true first path (FP). Nevertheless, the presence of the dense multipath and non-line-of-sight (NLOS) condition in indoor environments makes the FP detection quite challenging. No one denies that numerous achievements regarding these problems have previously been reported in the literature [12]–[16]; however, most of them do not scale because the detection of the FPs of multiple targets is quite complex and difficult to achieve. It is worth mentioning that the existing solutions consider the issue from another angle with the aim of avoiding interference and reducing the matter to a single target problem either by using a scheduled message exchange [17], [18] that is complex, energy consuming and requires a tight synchronization, or implementing different collision avoidance techniques [19]–[21] which significantly limit the number of supported targets.

Contributions, the present paper aims to contribute to the development of a new method that estimates the TOA of a number of targets without exchanging messages or using collision avoidance techniques. From mixed signals, the proposed approach uses: i) the singular value decomposition (SVD) to detect the FP of each target, and ii) a matched filter along with an iterative threshold crossing algorithm to determine the number of targets and estimate their TOAs. The suggested method is then validated using the CM1 channel model.

The remainder of this paper is structured as; Section 2 describes the UWB ranging system model. Next, section 3 provides the SVD theory along with the detailed steps of the proposed algorithm. Then, the corresponding simulation results are discussed in section 4; and finally, the last section 5 concludes the paper.

2. UWB RANGING SYSTEM MODEL

2.1. Ranging signal

In UWB ranging systems, short time pulse is commonly used because it provides a high time delay precision with low energy consumption. Due to the Federal Communications Commission's (FCC) regulations for UWB transmissions, the Gaussian pulse and its derivatives are commonly used in UWB ranging systems. Therefore, in this paper, the second derivative of the Gaussian pulse is employed as the UWB ranging signal, which can be expressed as:

$$s(t) = \frac{d^2y(t)}{dt^2} = \left(1 - 4\pi\frac{t^2}{\alpha^2}\right)\mathrm{e}^{\left(\frac{-2\pi t^2}{\alpha^2}\right)} \tag{1}$$

where $y(t)$ is the Gaussian pulse and is the α waveform shape factor.

2.2. Channel model

The IEEE 802.15.4a channel model [22] is the first international standard that defines a physical layer for accurate ranging and positioning applications. The IEEE 802.15.4a channel model provides different models for different frequency ranges: i) an UWB model from 2 to 10 GHz; ii) a body area network model from 2 to 6 GHz, and iii) an UWB model from 100 to 900 MHz; iv) a narrowband model for a 1 MHz carrier frequency. Moreover, as shown in Table 1, the IEEE 802.15.4a standard can be divided into eight channel models for different types of environments and line-of-sight (LOS)/NLOS conditions.

Table 1. Description of IEEE 802.15.4a channel models

Channel Model Number	Description
CM1	LOS of indoor residential (7-20 m)
CM2	NLOS of indoor residential (7-20 m)
CM3	LOS of indoor office (3-28 m)
CM4	NLOS of indoor office (3-28 m)
CM5	LOS of outdoor (5–17 m)
CM6	NLOS of outdoor (5–17 m)
CM7	LOS of industrial (2–8 m)
CM8	NLOS of industrial (2–8 m)

Considering our research interest, the IEEE 802.15.4a CM1 channel model is used to validate the proposed method. It should be noted that the IEEE 802.15.4a channel impulse response is based on a modified Saleh-Valenzuela model that follows a clustering structure. Moreover, the multipath components arrive in groups, called clusters. The cluster arrival times follow the poisson process, and within each cluster ray arrival times are modelled using a mixture of poisson processes. The mathematical form of the IEEE 802.15.4a channel impulse response is expressed as:

$$h(t) = \sum_{l=0}^{L} \sum_{k=0}^{K} \alpha_{k,l}\, e^{j\phi_{k,l}} \delta\left(t - T_l - \tau_{k,l}\right) \quad (2)$$

where L denotes the number of clusters and K the number of rays within each cluster; $\alpha_{k,l}$ is the multipath gain and $\phi_{k,l}$ the multipath phase distributed uniformly within the range [0 2π]; T_l is the delay of the lth cluster and $\tau_{k,l}$ is the delay of the kth ray in the lth cluster.

The received signal is expressed as:

$$r(t) = s(t) * h(t) + n(t) \quad (3)$$

where $s(t)$ is the UWB ranging signal, $h(t)$ is the channel impulse response and $n(t)$ is the additive white Gaussian noise; * denotes the convolution. Based on (1) and (2), the received signal can be written in:

$$r(t) = \sum_{l=0}^{L} \sum_{k=0}^{K} \alpha_{k,l}\, e^{j\phi_{k,l}} s\left(t - T_l - \tau_{k,l}\right) + n(t) \quad (4)$$

The signal received from multiple targets is given by:

$$R(t) = \sum_{j=1}^{J} r_j(t) \quad (5)$$

where $r_j(t)$ is the signal received form the jth target, and J is the total number of targets.

2.3. System performance

The root-mean-squared-error (RMSE) and the Cramer-Rao lower bound (CRLB) are calculated to evaluate the performance of our ranging system. It is worth noting that the RMSE, as given by (6), serves to assess the accuracy of the estimated TOA, and the CRLB, represented by (7) according to [23], is used to determine the accuracy limit of the distance estimation using the TOA method.

$$RMSE = \sqrt{\sum_{k=1}^{Ns} ((\tau_k - \tau_{TOA}) * c)^2 / Ns} \quad (6)$$

where τ_k is the estimated TOA of each realization; τ_{TOA} is the true TOA; c is the velocity of the electromagnetic wave and Ns represents the number of simulations.

$$V\{\hat{d}\} \geq \sqrt{\frac{c^2}{8\pi^2 \beta^2 SNR}} \quad (7)$$

Furthermore, it should be noted that $\hat{d}$ is the estimated distance using TOA method, and β is the effective bandwidth of the UWB ranging signal. One may clearly observe that, considering in (7), the distance estimation accuracy increases with the bandwidth, which justifies the use of UWB signals in ranging systems.

3. SVD-BASED TOA ESTIMATION FOR MULTIPLE TARGETS

3.1. SVD theory

Singular value decomposition is one of the most widely used techniques in numerical linear algebra to decompose a matrix into several component matrices. This procedure is frequently employed in data processing, dimensionality reduction, and as a foundation of machine learning [24], [25]. The SVD of a matrix $A \in \mathbb{C}^{n \times m}$ is a decomposition of the form $U\Sigma V^*$that always exists for any real or complex matrix. It is useful to note that $U \in \mathbb{C}^{n \times n}$ and $V \in \mathbb{C}^{m \times m}$ are unitary matrices and $\Sigma \in \mathbb{R}^{n \times m}$ is a diagonal matrix; the columns of $U$are the left singular vectors, the columns of $V$are the right singular vectors, and the diagonal elements of Σ are the singular values $\sigma_i$such that ($\sigma_1 \geq \cdots \geq \sigma_m \geq 0$).

3.2. Proposed method

In this paper, the following scenario is considered Figure 1. The ranging signals are emitted by the targets (one-way ranging) with a perfect synchronization between the transmitters and the receiver. A line-of-sight (LOS) is guaranteed and the channel is taken as time-invariant during the observation time. The number of targets is four and the minimum delay between the ranging signals is set to 2 ns.

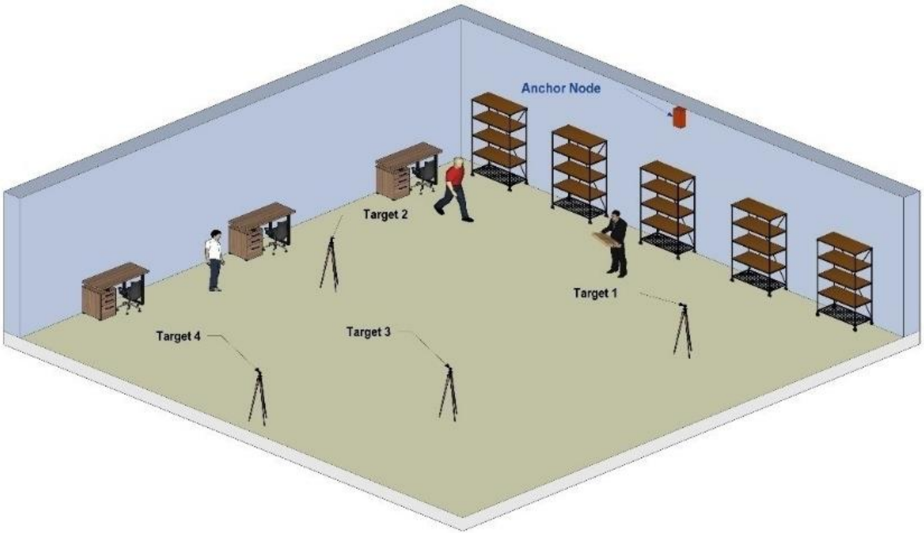

Figure 1. The proposed scenario

The key to TOA-based ranging is to detect the FP and to estimate its TOA. The proposed method uses the SVD to find the FP of each target, and subsequently a matched filter, combined with an iterative threshold crossing algorithm, is deployed to determine the number of targets and estimate their FP TOAs. The flow chart of the proposed method is presented in Figure 2.

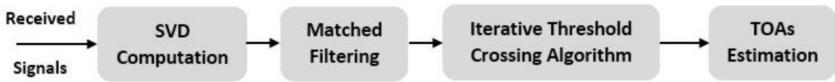

Figure 2. Flow chart of the proposed method

The received signals can be expressed as a $R^{K\times N}$matrix:

$$R = \begin{bmatrix} \vdots & \vdots & & \vdots \\ R_1 & R_2 & \cdots & R_N \\ \vdots & \vdots & & \vdots \end{bmatrix} \tag{8}$$

where each column of the $R^{K\times N}$matrix represents a frame, and each frame contains a mixture of signals arriving from different targets. First, the SVD of the matrix $R^{K\times N}$ is computed as (9).

$$R = U\Sigma V^* \tag{9}$$

As mentioned above, the channel is time-invariant during the observation time. The FPs are therefore fixed among all frames. Moreover, the left singular vectors are hierarchically arranged in terms of how much correlation they capture in the columns of R, thus, the first left singular vector is the most dominant correlation vector. This implies that the correlated paths among the columns of R appear with a higher amplitude in the first left singular vector. Since the FPs are fixed, then the correlated paths are the FPs of the corresponding targets. An illustration of the process is given in Figure 3, where the received signals are represented in Figure 3(a) and the first left singular vector is represented in Figure 3(b).

Afterwards, the first left singular vector is put into a matched filter and then squared to maximize its SNR, the output denoted as V_k is passed to the iterative threshold crossing algorithm to determine the number of targets and estimate the corresponding FP TOA. To do this, a threshold is first required. Note that the proposed method does not require a detailed study to find the threshold value. Therefore, for the simplicity of implementation, the threshold is set to $\eta = \lambda\sigma$, where λ is a constant and σ is the standard deviation of the first left singular vector. In addition, for the purpose of determining the proper value of the constant λ, the averaged RMSE, as given by (10), is calculated for different values of λ. Moreover, CM1 is used as a channel model, Ns is set to 100 simulations, and the SNR is increased from -10 to 20 dB in steps of 5 dB.

$$RMSE_{avg} = \frac{1}{L}\sum_{l=1}^{L} RMSE_l\,, l = 1, 2, \dots L \quad (10)$$

where L is the total number of targets and $RMSE_l$ is the TOA estimation RMSE of the lth target.

The results presented in Figure 4 prove that the proposed method does not require a detailed study to find the threshold value. As seen in Figure 4, in all cases the averaged RMSE decreases until it reaches its lowest point at $\lambda = 0.5$, from which it starts to increase at different rates depending on the signal-to-noise ratio (SNR) value. The averaged RMSE reaches its lowest at $\lambda = 0.5$, hence, λ can be set to 0.5.

The generic pseudo-code for the iterative threshold crossing algorithm is given in Algorithm 1. First, the V_k samples are compared to the threshold η and the TOA of the first target is obtained as a function of the first threshold crossing sample index TC_1. In the first iteration, given that the minimum delay between targets ranging signals is 2 ns, the samples starting from $TC_1 + S$ are compared to the threshold η and the TOA of the second target is calculated as a function of the first threshold crossing sample TC_2, with $S = \tau_{min}/T_s$; note that τ_{min} and T_s are the minimum delay and the sampling interval, respectively. Similarly, in the second iteration, the samples starting from $TC_2 + S$ are compared to the threshold η and so on. The algorithm stops when there are no samples exceeding the threshold.

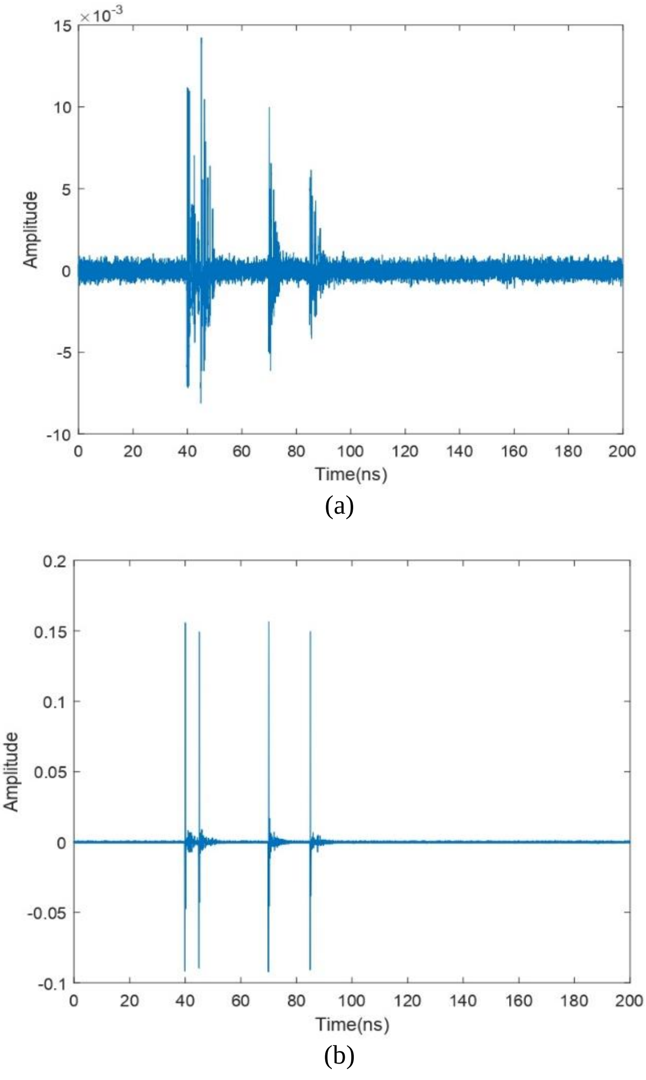

Figure 3. Illustartion of the extracted FPs (CM1 channel, SNR=10 dB) (a) received signals and (b) first left singular vector

Algorithm 1. The generic iterative threshold crossing algorithm for multiple targets

Input:
$V_{1:K} = (V_1, V_2, \dots, V_K)$
Threshold η
Initialise:
The number of TC samples $L = 0$
Counter $j = 1$
The first TC sample index $TC_j = First\{k|V_k > \eta\}$
$S = \tau_{min}/T_s$
Iterate: while $(TC_j \neq NULL)$
Increment the counter $j = j + 1$
Calculate the next TC sample index $TC_j = First\left\{k|V_{(TC_{j-1}+S):K} > \eta\right\}$
Output:
The number of TC samples $L = j - 1$
The recorded indexes of the TC samples $TC_{1:L} = (TC_1, TC_2, \dots, TC_L)$

Finally, the targets TOAs can be calculated using the expression:

$$\hat{t}_{toa_l} = TC_l T_s - \tau_{guard}, l = 1,2, \dots, L \quad (11)$$

where τ_{guard} is the guard interval.

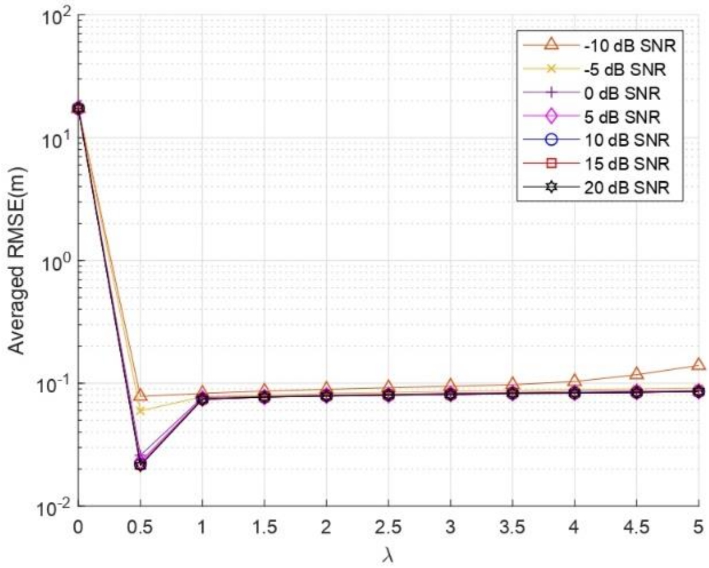

Figure 4. Averaged RMSE as a function of λ

4. SIMULATION RESULTS AND DISCUSSION

The proposed method is tested by means of the IEEE 802.15.4a CM1 channel model. The results presented in Figure 5 are obtained under the following parameters: the UWB ranging signal used is the Gaussian doublet with a pulse duration of 1 ns, λ is set to 0.5 and the number of frames $N = 300$ frames with a frame duration of 200 ns. The SNR ranged from -10 to 20 dB, with a step of 5 dB; the number of targets is 4 and Ns of the RMSE is set to 100 simulations.

Figure 5 shows that the proposed method achieves a ranging error of a few centimeters without using collision avoidance techniques or exchanging messages. However, there is still a significant difference with the best theoretically attainable accuracy (CLRB) (the black line in Figure 5), particularly at high SNR (> 0dB). In addition, the ranging error of the first target in Figure 5(a) is less than the ranging errors of the other three targets in Figures 5(b) to 5(d). This is due to the fact that the first target's FP does not interfere with the multipath components of the signals arriving from the other three targets, indicating that the FP of the first target among all frames of the received signals is highly correlated in comparison to the FPs of the other three targets and can thus be extracted precisely by the SVD.

Furthermore, to prove the effectiveness of our proposed method, its performance is compared to that of the energy detection (ED)-based methods such as maximum energy selection method (MES) and threshold crossing (TC) method [13], [26]. These methods are based on an energy detection receiver, which squares the received signal and feeds it into a finite time integrator to calculate its energy. The MES method selects the maximum energy block as the FP, whereas the TC method selects the first threshold crossing energy block as the FP; for the TC method, the normalized threshold given in (12) is used to compute the threshold value. The normalized threshold is stated for a given maximum and minimum energy value as (12).

$$\eta_{norm} = \frac{\eta - \min\{E_n\}}{\max\{E_n\} - \min\{E_n\}} \quad (12)$$

Because the ED-based techniques are intended for single target FP TOA estimation, the performance of the FP TOA estimation of each of the four targets is compared with that achieved by the ED-based methods for a single target during the comparison process. According to the simulations done in [26], the normalized threshold is set to 0.6, the energy block width is set to 4 ns and the remaining parameters are the same as indicated previously. It can be seen from Figure 6 that the RMSE of the FP TOA estimation of each target is better than that obtained by the ED-based approaches. The FP TOA estimation accuracy of the ED-based technique is limited; at high SNR (> 5 dB) it hits an error floor induced by the integration interval of the ED-receiver.

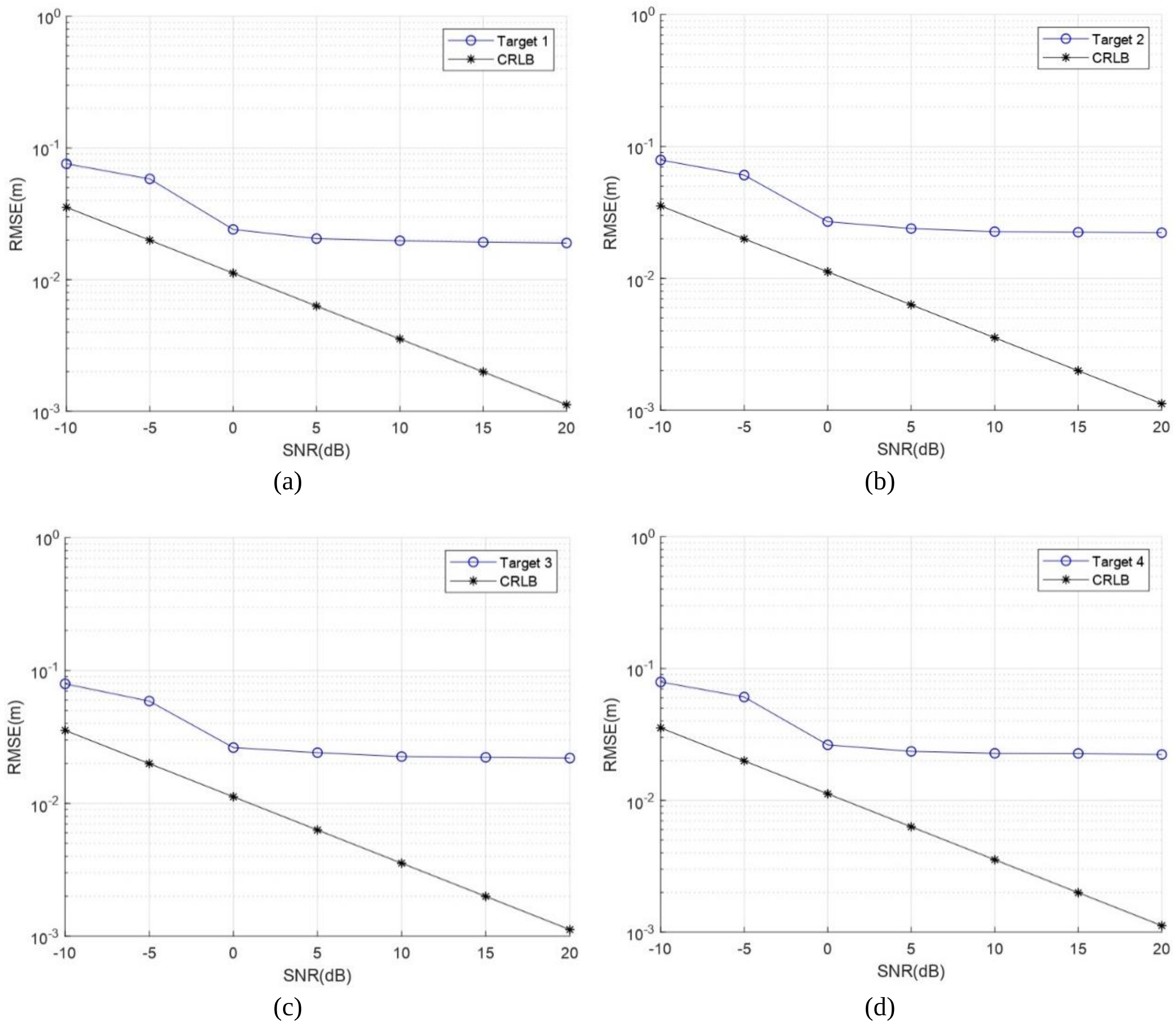

Figure 5. TOA estimation performance of the proposed method: (a) Target 1, (b) Target 2, (c) Target 3, and (d) Target 4

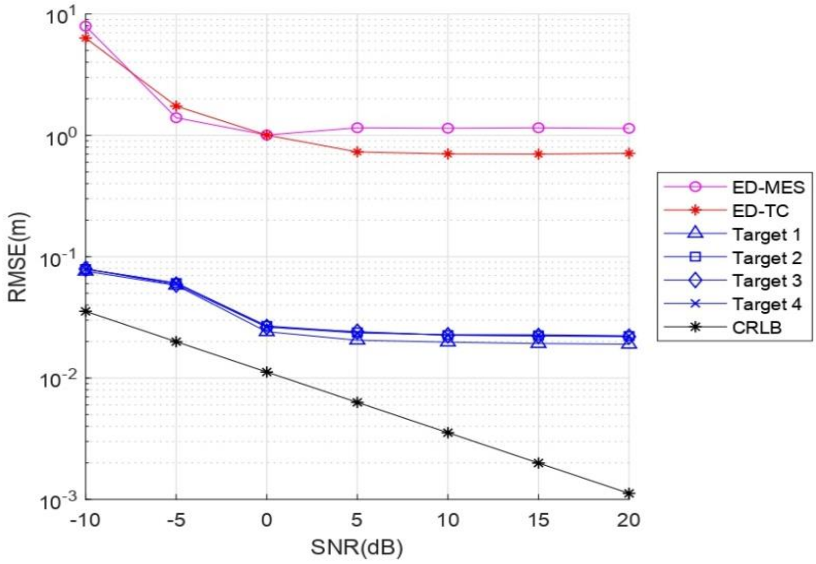

Figure 6. Performance comparison of the proposed method

5. CONCLUSION

The novel SVD-based TOA estimation algorithm for multiple targets presented in this paper represents a departure from the existing approaches; it leads to better performance and allows reducing the complexity of calculations by avoiding the use of complex collision avoidance techniques. The SVD is used to find the FP of the targets, and the TOA is determined by performing a matched filtering in combination with an iterative threshold crossing algorithm. The simulation results obtained using the CM1 IEEE 802.15.4a channel model helped to verify the effectiveness and robustness of the proposed approach. This work will certainly stimulate future research on the use of SVD in other signal processing-related problems.

REFERENCES

[1] R. F. Brena, J. P. G. Vázquez, C. E. G. Tejada, D. M. Rodriguez, C. V. Rosales, and J. Fangmeyer, "Evolution of indoor positioning technologies: a survey," *Journal of Sensors*, vol. 2017, pp. 1–21, 2017, doi: 10.1155/2017/2630413.
[2] K. Al Nuaimi and H. Kamel, "A survey of indoor positioning systems and algorithms," in *2011 International Conference on Innovations in Information Technology, IIT 2011*, 2011, pp. 185–190, doi: 10.1109/INNOVATIONS.2011.5893813.
[3] J. Xiao, Z. Zhou, Y. Yi, and L. M. Ni, "A survey on wireless indoor localization from the device perspective," *ACM Computing Surveys*, vol. 49, no. 2, pp. 1–31, Nov. 2016, doi: 10.1145/2933232.
[4] A. Alarifi *et al*., "Ultra wideband indoor positioning technologies: Analysis and recent advances," *Sensors (Switzerland)*, vol. 16, no. 5, p. 707, May 2016, doi: 10.3390/s16050707.
[5] V. T. Quang and T. Ho-Sy, "Maximum convergence algorithm for WiFi based indoor positioning system," *International Journal of Electrical and Computer Engineering*, vol. 11, no. 5, pp. 4027–4036, Oct. 2021, doi: 10.11591/ijece.v11i5.pp4027-4036.
[6] M. S. Rahman, M. M. Haque, and K.-D. Kim, "Indoor positioning by LED visible light communication and image sensors," *International Journal of Electrical and Computer Engineering (IJECE)*, vol. 1, no. 2, p. 161, Nov. 2011, doi: 10.11591/ijece.v1i2.165.
[7] F. Mazhar, M. G. Khan, and B. Sällberg, "Precise indoor positioning using UWB: a review of methods, algorithms and implementations," *Wireless Personal Communications*, vol. 97, no. 3, pp. 4467-4491, 2017, doi: 10.1007/s11277-017-4734-x.
[8] I. Guvenc, S. Gezici, and Z. Sahinoglu, "Ultra-wideband range estimation: Theoretical limits and practical algorithms," in *Proceeedings of The 2008 IEEE International Conference on Ultra-Wideband, ICUWB 2008*, Sep. 2008, vol. 3, pp. 93–96, doi: 10.1109/ICUWB.2008.4653424.
[9] S. Gezici and H. V. Poor, "Position estimation via ultra-wide-band signals," Proceedings of the IEEE, vol. 97, no. 2, pp. 386–403, Feb. 2009, doi: 10.1109/JPROC.2008.2008840.
[10] S. Aditya, A. F. Molisch, and H. M. Behairy, "A survey on the impact of multipath on wideband time-of-arrival based localization," *Proceedings of the IEEE*, vol. 106, no. 7, pp. 1183–1203, Jul. 2018, doi: 10.1109/JPROC.2018.2819638.
[11] S. Gezici *et al*., "Localization via ultra-wideband radios: A look at positioning aspects of future sensor networks," *IEEE Signal Processing Magazine*, vol. 22, no. 4, pp. 70–84, Jul. 2005, doi: 10.1109/MSP.2005.1458289.
[12] J. Li, X. Cui, H. Song, Z. Li, and J. Liu, "Threshold selection method for UWB TOA estimation based on wavelet decomposition and kurtosis analysis," *Eurasip Journal on Wireless Communications and Networking*, vol. 2017, no. 1, p. 202, Dec. 2017, doi: 10.1186/s13638-017-0990-4.
[13] W. Liu and X. Huang, "Analysis of energy detection receiver for TOA estimation in IR UWB ranging and a novel TOA estimation approach," *Journal of Electromagnetic Waves and Applications*, vol. 28, no. 1, pp. 49–63, Jan. 2014, doi: 10.1080/09205071.2013.855149.
[14] Z. Yin, K. Cui, Z. Wu, and L. Yin, "Entropy-based TOA estimation and SVM-based ranging error mitigation in UWB ranging systems," *Sensors (Switzerland)*, vol. 15, no. 5, pp. 11701–11724, May 2015, doi: 10.3390/s150511701.

[15] L. Zhang, C. Song, and W. Sheng, “Time delay estimation based on double dynamic threshold in indoor multipath environment,” in *ICEIEC 2019 - Proceedings of 2019 IEEE 9th International Conference on Electronics Information and Emergency Communication*, Jul. 2019, pp. 32–35, doi: 10.1109/ICEIEC.2019.8784467.

[16] W. Liu, H. Ding, X. Huang, and Z. Liu, “TOA estimation in IR UWB ranging with energy detection receiver using received signal characteristics,” *IEEE Communications Letters*, vol. 16, no. 5, pp. 738–741, May 2012, doi: 10.1109/LCOMM.2012.030912.112445.

[17] B. Kempke, P. Pannuto, B. Campbell, and P. Dutta, “Sure point: Exploiting ultra wideband flooding and diversity to provide robust, scalable, high-fidelity indoor localization,” in *Proceedings of the 14th ACM Conference on Embedded Networked Sensor Systems, SenSys 2016*, Nov. 2016, pp. 137–149, doi: 10.1145/2994551.2994570.

[18] Y. Qin, F. Wang, and C. Zhou, “A distributed UWB-based localization system in underground mines,” *Journal of Networks*, vol. 10, no. 3, p. 134, Apr. 2015, doi: 10.4304/jnw.10.3.134-140.

[19] N. C. Rowe, A. E. Fathy, M. J. Kuhn, and M. R. Mahfouz, “A UWB transmit-only based scheme for multi-tag support in a millimeter accuracy localization system,” in *WiSNet 2013 - Proceedings: 2013 IEEE Topical Conference on Wireless Sensors and Sensor Networks - 2013 IEEE Radio and Wireless Week, RWW 2013*, Jan. 2013, pp. 7–9, doi: 10.1109/WiSNet.2013.6488616.

[20] J. Tiemann, F. Eckermann, and C. Wietfeld, “ATLAS-an open-source TDOA-based ultra-wideband localization system,” in *2016 International Conference on Indoor Positioning and Indoor Navigation, IPIN 2016*, Oct. 2016, pp. 1–6, doi: 10.1109/IPIN.2016.7743707.

[21] M. Ridolfi, S. van de Velde, H. Steendam, and E. De Poorter, “Analysis of the scalability of UWB indoor localization solutions for high user densities,” *Sensors (Switzerland)*, vol. 18, no. 6, p. 1875, Jun. 2018, doi: 10.3390/s18061875.

[22] A. F. Molisch *et al*., “IEEE 802.15. 4a channel model-final report,” *Ieee P*, vol. 15, pp. 802.1504--0662, 2006, [Online]. Available: https://mentor.ieee.org/802.15/file/04/15-04-0662-00-004a-channel-model-final-report-r1.pdf.

[23] D. Dardari, A. Conti, U. Ferner, A. Giorgetti, and M. Z. Win, “Ranging with ultrawide bandwidth signals in multipath environments,” *Proceedings of the IEEE*, vol. 97, no. 2, pp. 404–425, Feb. 2009, doi: 10.1109/JPROC.2008.2008846.

[24] T. Peters, “Data-driven science and engineering: machine learning, dynamical systems, and control: by SL Brunton and JN Kutz, 2019, Cambridge, Cambridge University Press, 472 pp.,£49.99 (hardback), ISBN 9781108422093. Level: postgraduate. Scope: textbook.” Taylor\& Francis, 2019.

[25] K. Baker, “Singular value decomposition tutorial,” Thesis, The Ohio State University, 2005.

[26] I. Guvenc and Z. Sahinoglu, “Threshold-based TOA estimation for impulse radio UWB systems,” in *ICU 2005: 2005 IEEE International Conference on Ultra-Wideband, Conference Proceedings*, 2005, vol. 2005, pp. 420–425, doi: 10.1109/icu.2005.1570024.

BIOGRAPHIES OF AUTHORS

Ibrahim Yassine Nouali received his Master degree in Telecommunication at the University of Tlemcen, (Algeria) in 2018. Currently he is a PhD student at the same University and a member of STIC laboratory. His doctoral research center around ultra wide band technology and indoor positioning techniques. He can be contacted at email: ibrahimyassine.nouali@univ-tlemcen.dz and nouali.ibrahim.yassine01@gmail.com.

Zohra Slimane received Magister Diploma (2008), Ph.D. (2012) and HDR (2017), in Telecommunication from Tlemcen University (Algeria). Since 2008, she has been researcher at STIC Laboratory and system engineer at Sonatrach Aval Research Group. In 2014, she joined Belhadj Bouchaib University Center (Algeria), where she is currently an associate and research Professor, responsible for LMD graduation and doctorate training in the telecommunications sector. Since 2019, she has been involved as project leader dedicated to indoor localization. Her research interests include location and imaging radars, UWB sensors, networking, mobile networks, ubiquitous internet and next-generation networks. She can be contacted at email: zohra.slimane@univ-temouchent.edu.dz and zoh_slimani@yahoo.fr.

Abdelhafid Abdelmalek received the Laurea degree in Telecommunication Engineering from Institute of Telecommunications Oran (Algeria) in 1991, and Diploma of deepened studies in optoelectronic at Nancy (France) in 1993. From 1994 to 2000, he worked as engineer in charge of design and management of ISDN networks at Algerie Telecoms Company. In 2002, he received Magister Diploma in Signals and systems at Tlemcen University, Algeria. He subsequently joined the faculty of technology and STIC Laboratory as research Professor. He received the Ph.D degree in Electronics in 2013. He has participated in several national research frameworks and projects. His main research activities cover radar, data communications, mobile networks, security, protocols and high-speed optical networks. He can be contacted at email: abdelmalekabdelhafid@gmail.com.